Iranian Journal of Oil & Gas Science and Technology, Vol. 8 (2019), No. 4, pp. 106-121
http://ijogst.put.ac.ir

Influence of Pipeline Operating Pressure on Value Setting of Automatic Control Valves at Different Pressure Drop Rates

Mehdi Mahmoodi[1] and Mofid Gorji Bandpy[2*]

[1] Ph.D. Candidate, Babol Noshirvani University of Technology, Mazandaran, Iran
[2] Professor, Babol Noshirvani University of Technology, Mazandaran, Iran

Received: November 12, 2017; *revised*: January 17, 2018; *accepted*: February 25, 2018

Abstract

When a natural gas pipeline ruptures, the adjacent upstream and downstream automatic control valves (ACV) should close quickly to prevent leakage or explosion. The differential pressure set point (DPS) at each valve location is the main criteria for value setting in ACV actions. If the DPS is not properly adjusted, the ACV may mistakenly close or it may not take any actions at a proper time. In this study, the effect of characteristic parameters such as pipeline operational pressure (POP) and pipeline pressure drop rate (ROD) due to rupture or a major leak was experimentally investigated on DPS. 25 different conditions with the double set of the mentioned typical characteristic parameters were chosen. In each condition, the differential pressure (DP) was measured over a period of 180 s by statistically analyzing the experimental results, so 25 maximum DP values (DPSs) were obtained. The DPS rises by an increase in ROD or a decrease in POP. Because of using nitrogen gas instead of natural gas for safety reasons and the uncertainties, the DPS results can be practically applied by adding a safety factor of 15%. Finally, the diagram of DPS with respect to ROD and that of non-dimensional DPS (DOP) versus non-dimensional ROD (RTP) were provided for different POP's.

Keywords: Automatic Control Valve, Gas Pipelines, Operating Pressure, Pressure Drop Rate

1. Introduction

Pipelines are used broadly all over the world for transportation and distribution of water, natural gas, and other light petroleum products. Natural gas and petroleum products are carried over long distances from oil and gas fields or refineries to customers. Rupture, explosion, or a large leak due to various reasons are hazardous problems affecting the safe operation of pipelines. Leak detection in pipeline systems carrying natural gas and other petroleum products is critically serious from the point of view of economic, environment, and safety aspects. The hardware-based methods such as pigging, acoustic methods, gas tracer, and radar methods are difficult to install (Geiger et al., 2003) and the software-based methods for continuously monitoring leaks are so expensive. ACV's are installed on oil and gas pipelines for these reasons. When a natural gas pipeline ruptures, the automatic control valves should close quickly to prevent significant gas leakage before the rupture causes a disastrous accident.

Various experimental studies have been performed on leak detection in liquid pipelines (Souza et al., 2000; Brunone and Ferrante, 2002) and gas pipelines (Mahmoodi et al., 2017), but relatively fewer

* Corresponding author:
Email: gorji@nit.ac.ir

studies have been presented on gas pipelines. Leak tests on gas pipeline simulator were conducted by acoustic-based methods in laboratory (Watanabe and Himmelblau, 1980). A field study on a 150-km long gas pipeline has also been reported (Billmann and Isermann, 1984). Several studies on leak detection (Noguerol, 2011; Harriott, 2011, Reddy et al., 2011, Yan et al., 2015; Ebrahimi, 2016, Chen et al., 2017; Mahmoodi et al., 2018) and rupture detection (Peekema, 2013; Richards, 2013) in gas pipelines have been reported. However, there are only a few studies on setting the differential pressure set point (DPS) value of automatic control valves (ACVs) (Lorusso, 2012; Doostaregan, 2013; Wang, 2013; Zuo, 2015), especially about how the value settings might differ between gas pipelines.

The DPS value is the important parameter that determines whether an ACV closes in time or not. The calculation of DPS values of ACV's is complex owing to the changing operating conditions along a pipeline. The normal pressure drop rate is due to frictional losses in a piping system. The normal pressure drop should not cause an ACV to act. Actually, the differential pressure value between two sides (the right and left) of the diaphragm in a differential pressure switch (see Figure 1) is DP. When the DP value equals the DPS, the diaphragm moves to the right and changes the normally closed valve position. ACV will be regulated at a certain DPS in different conditions. The DP value depends on several parameters such as pipeline operating pressure (POP) and the rate of pressure drop due to rupture or a large leak (ROD). The orifice diameter (see Figure 1) is another important parameter of ACV's. The orifice diameter is considered to be constant and equal to 0.5 mm in this study. As mentioned, the DPS's of ACV's are usually adapted based on experiments or the estimated values derived from the pipeline steady flow over a long time.

In this study, the effects of critical parameters such as POP and ROD on the DPS of ACV's were experimentally studied. 25 different typical conditions were chosen with the double set of the mentioned parameters. Each condition was experimentally studied 3 times, so 75 tests were performed. The DP over a period of 180 s in each condition was depicted by the statistical analysis of the experimental results; therefore, 25 DPS's with their occurrence times were obtained. A series of equations relating the DP value over 180 s to the time at different POP's and ROD's were developed. An uncertainty analysis was also performed, and finally a series of equations correlating the DOP with the RTP at different POP's were extracted. The dimensionless DPS and ROD are named DOP and RTP respectively.

2. Experimental test setup

A schematic of the experimental test setup is depicted in Figure 1, and the utilized facilities are illustrated in Figure 2. The gaseous fluid is transferred from pipeline to ACV through a connecting hose and tube (No. 19 and No. 20 in Figure 3)< which is divided into three branched tube routes; Route 1 is through the normally closed valve (NC Valve in Figure 1). The test setup is shown in Figure 2 and it includes: (1) pipeline, (2) a compressed nitrogen cylinder, (3) a pressure gauge, (4) a pressure diaphragm switch, (5) an electrical box, (6) a PT signal receiver, (7) a pressure transducer (PT), (8) a set of orifice and check valve, (9) a reference tank, (10) tubing, (11) a calibrated valve, and (12) a connecting hose. A closed-ends pipe was used as the pipeline (No. 1 in Figure 2). To avoid any hazardous conditions, nitrogen gas was used instead of natural gas. The pipeline pressure is attained at the desired POP by a compressed nitrogen cylinder (No. 2 in Figure 2). A calibrated valve (No. 11 in Figure 2) is attached to the pipeline to create an ROD by withdrawing gas and releasing it to the atmosphere.

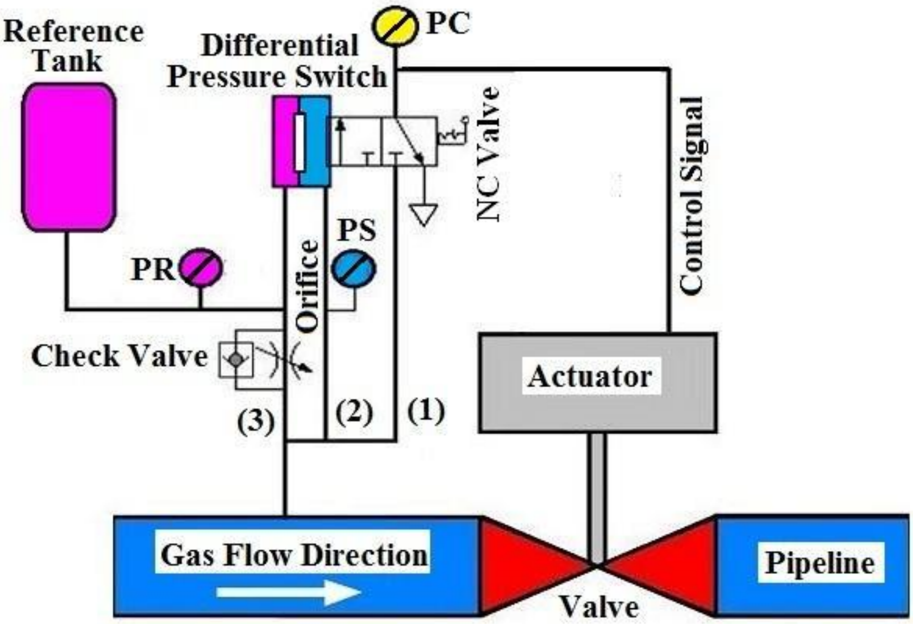

Figure 1

A schematic of the experimental test setup.

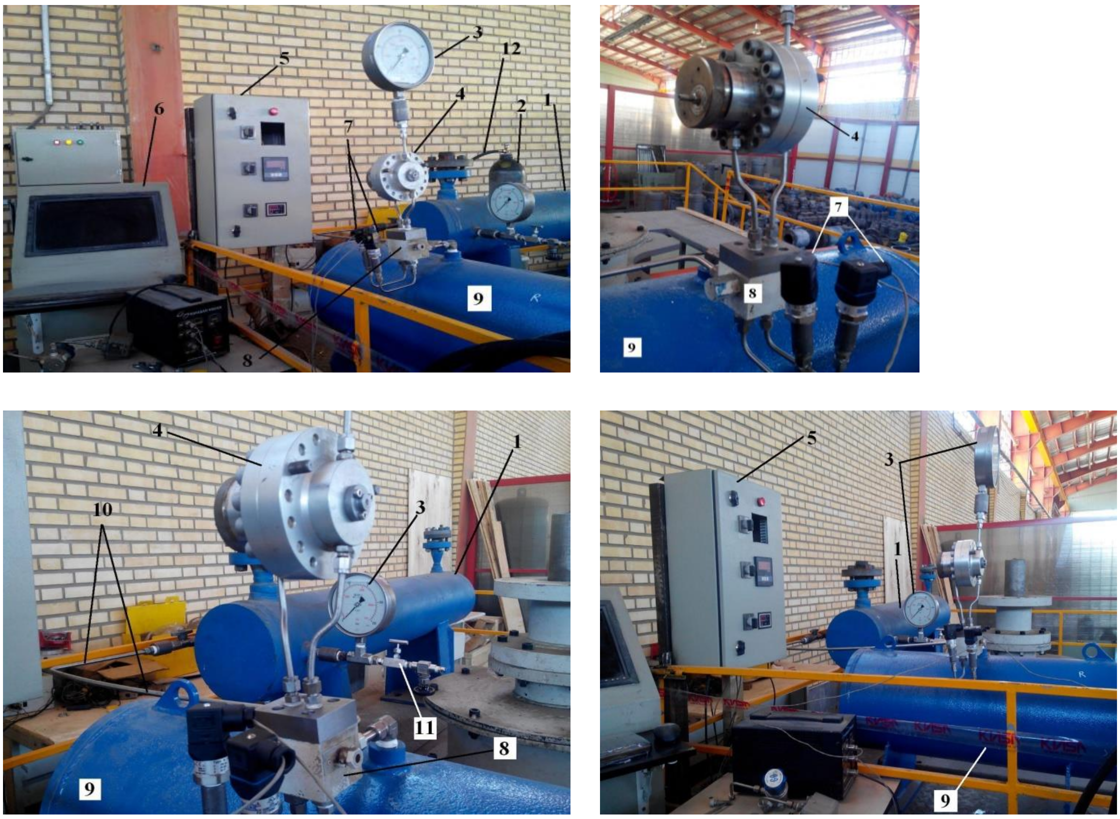

Figure 2

The experimental test setup.

Nitrogen gas enters the reference tank by means of a set of orifice and check valves (No. 8 in Figure 2) installed in Route 3 (Figure 1). The pressure of the reference tank equals the pipeline pressure instantaneously. When a failure occurs in the pipeline, the reference tank pressure will be greater than the pipeline pressure. Now, the route with the check valve is closed. Therefore, all the fluid in the reference tank passes through the orifice. This creates a new pressure drop rate in the system which is lower than the ROD. The DP between the pipeline and the reference tank equals the DP between the two sides of the diaphragm in the differential pressure switch. The normally closed valve position changes when the DP attains the maximum value (i.e. DPS) at the time of $t_{max,}$ and finally ACV acts.

The isolated pipeline is pressurized to a constant value, and the pressure is then reduced for 5 minutes by opening the valve (No. 11 in Figure 2) which is installed on the pipeline. The mean ROD (kPa/s) should be measured for this determined valve opening (in degree). To calculate the ROD, the pressure difference (kPa) between the initial time and 5 minutes after the valve opens was divided by 300 seconds. Therefore, the ROD was obtained for this determined valve opening. Consequently, the valve calibration was performed in all the conditions. Finally, the valve was calibrated for 9 ROD's from 0.2 kPa/s up to 2 kPa/s. 25 different typical conditions are summarized in Table 1. Each condition was experimentally studied 3 times, so 75 experimental tests were carried out. The maximum and minimum limits of each range of ROD depend on POP and the chosen orifice diameter. 25 DPS's with their occurrence times were obtained. The pieces of equipment used in this study are listed along with their uncertainties and measured parameters in Table 2.

Table 1

Experimental parameters and their values.

Parameter	Unit	Values
POP	kPa	3500, 5000, 7500, 9000, and 10500
ROD	kPa/s	0.2, 0.4, 0.6, 0.8, 1, 1.2, 1.4, 1.6, and 2

Table 2

Pieces of equipment and their uncertainties

Equipment and model	Accuracy	Measured section	Test range	Uncertainty in experiment
LCD digital stopwatch (Sigma-Aldrich, Germany)	± 0.003%	Time, ROD	0-180 s	$\pm 5.4\times10^{-3}$ s
Pressure transducer, PXM01MD0-160BARG5T (Omega, the UK)	± 0.05%	POP, DP, DPS, ROD	2060-10500 kPa	± 0.22% (± 8 kPa)

3. Results and discussion

As mentioned above, the DPS can be determined according to the maximum DP values over a period of 180 s. Failure occurred at the initial time (t=0) by ROD. The DP increased with respect to time to a maximum value (i.e., DPS), and then it dropped in all the conditions. The DP with respect to time is depicted based on the transmitted data by two pressure transducers, namely PTS and PTR, for 180 s after line-failure in each condition as displayed in Figures 3 to 7; The DP has been measured every 10 s. The DP is determined as a function of the ROD and the POP parameters and predicted by Equation 2 over a period of 180 s in all the conditions. Each condition has its six unique constant coefficients tabulated in Tables 3, 5, 7, 9, and 11.

$$DP = ae^{bt} + c\,ln\left(1 + dt\right) + et^2 + f \tag{1}$$

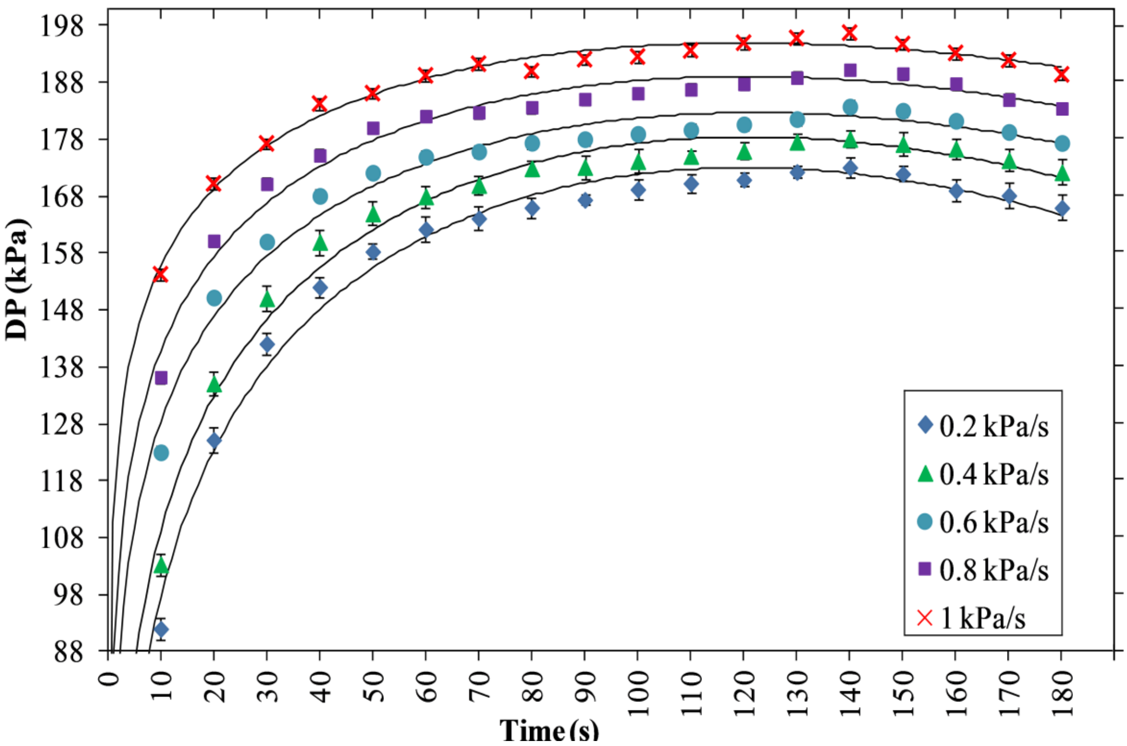

Figure 3

DP versus time for a POP of 3500 kPa.

Table 3

Coefficients of Equation 1 for a POP of 3500 kPa.

ROD	*a*	*b*	*c*	*d*	*e*	*f*
0.2	1.56×10^2	-2.84×10^6	3.8×10	7.72×10	-1.31×10^{-3}	-1.56×10^2
0.4	2.12×10^2	-2.84×10^6	3.47×10	1.04×10^3	-1.18×10^{-3}	-2.12×10^2
0.6	1.29×10^2	-2.84×10^6	2.71×10	1.32×10^3	-9.2×10^{-4}	-1.29×10^2
0.8	4.15×10^2	-2.84×10^6	2.43×10	1.83×10^2	-8.38×10^{-4}	-4.15×10
1	3.9×10	-2.84×10^6	1.97×10	2.01×10^3	-6.81×10^{-4}	-3.9×10

Each row in these tables is the result in each condition after 3 times of repetition. For data x_i, deviation is defined by d_i (Equation 2). The standard deviation (SD) is calculated by Equation 3. For parameter x, the uncertainty of the experimental test repetition and the uncertainty of its measuring equipment are shown by U_{rep} and U_{tool} respectively. The total uncertainty of each experimental test (U_{tot}) is defined by Equation 4, where, h_a is the half measuring equipment accuracy.

$$\bar{X} = \sum_{i=1}^{n} \frac{x_i}{n}$$
$$d_i = x_i - \bar{X} \qquad (2)$$
$$\sum_{i=1}^{n} d_i = 0$$

$$SD = \sqrt{\frac{\sum_{i=1}^{n} d_i^2}{(n-1)}} \tag{3}$$

$$U_{tot} = \sqrt{U_{tool}^2 + U_{rep}^2} = \sqrt{\frac{h_a^2}{3} + \frac{\sum_{i=1}^{n} d_i^2}{n(n-1)}} \tag{4}$$

The mean and maximum values of the standard deviation are 1.65 and 4.49 kPa respectively. Furthermore, the mean and maximum values of the DP estimation error are 1.03% and 5.74% respectively. The mean and maximum values of the DP total uncertainty are also 0.928 and 1.39 kPa, and the mean estimation error of t_{max} is 13.19% at a POP of 3500 kPa.

Table 4

t_{max} at a POP of 3500 kPa.

ROD	0.2	0.4	0.6	0.8	1
Estimated value	122	123	126	120	120
Estimation error	12.86%	12.14%	10%	14.29%	16.67%

The percent error of the DP estimation is defined using Equation 5. Its maximum and average values are presented in any conditions in Table 13. In any conditions, the estimated value of the DP is in good agreement with its obtained experimental value.

$$\text{Estimation error (\%)} = \frac{|\text{Estimated value - Experimental value}|}{\text{Experimental value}} \times 100 \tag{5}$$

According to the experimental tests, the required time to attain the maximum DP (t_{max}) is 140 seconds. The estimated value of t_{max} is calculated by solving Equation 6 which is the derivation of Equation 5. The estimated values of t_{max} and their errors are presented in Tables 4, 6, 8, 10, and 12 for each condition.

$$abe^{bt} + \frac{(c \times d)}{(1 + dt)} + 2et = 0 \tag{6}$$

When the POP is constant, the only variable parameter is ROD. An increase in ROD raises the DP when other parameters are kept constant (POP) in all the conditions. A more mass of compressed nitrogen gas in the pipeline ($\dot{m}_{PL}$) is discharged to atmosphere by increasing the ROD. The pressure of ACV equals the pipeline pressure at the initial time before pipeline failure. The pressure drop rate on the right side of the diaphragm in differential pressure switch (Figure 1) equals the ROD due to the direct connection. However, the pressure drop rate on the left side of the diaphragm in differential pressure switch differs from the ROD owing to the compressed nitrogen gas passing through the orifice. The mean and maximum values of the standard deviation are 1.72 and 3.36 kPa respectively; the mean and maximum values of the DP estimation error are 0.86% and 3.2% respectively.

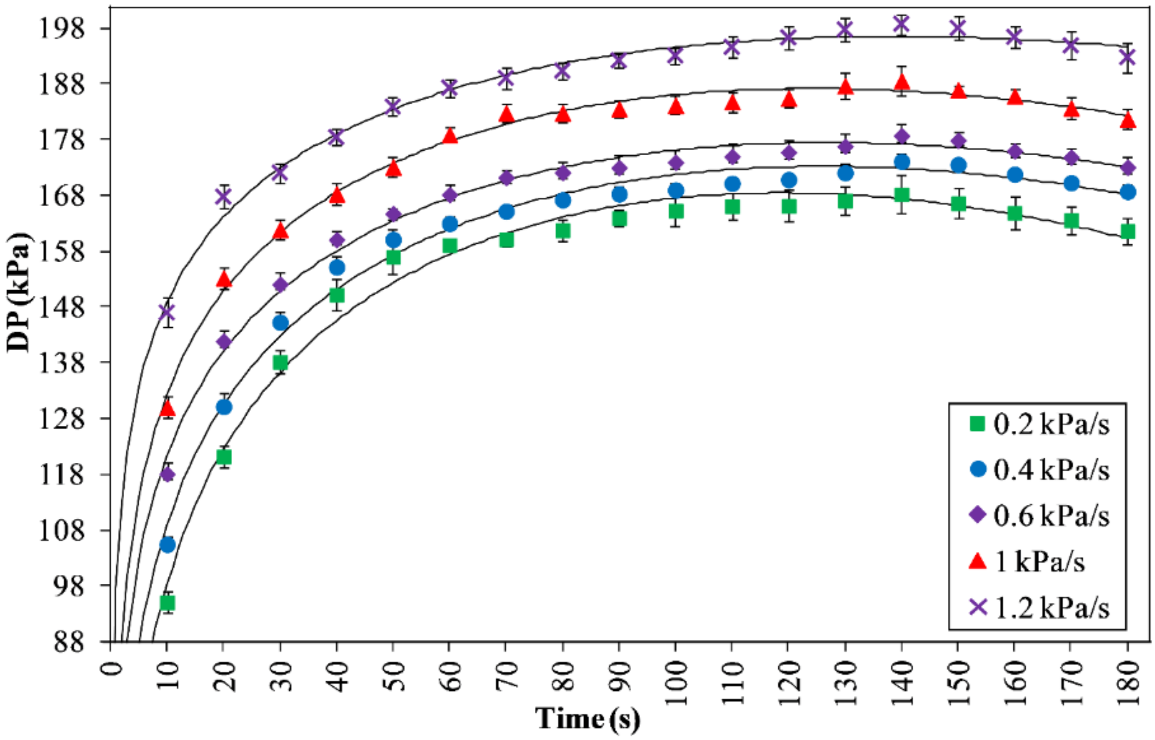

Figure 4

The DP versus time at a POP of 5000 kPa.

Table 5

Coefficients of Equation 1 at a POP of 5000 kPa.

ROD	***a***	***b***	***c***	***d***	***e***	***f***
0.2	2.53×10^{2}	-2.84×10^{6}	3.55×10	2×10^{3}	-1.25×10^{-3}	-2.53×10^{2}
0.4	2.04×10^{2}	-2.84×10^{6}	3.16×10	2.01×10^{3}	-9.92×10^{-4}	-2.04×10^{2}
0.6	1.52×10^{2}	-2.84×10^{6}	2.75×10	2.01×10^{3}	-8.55×10^{-4}	-1.52×10^{2}
1	1.37×10^{2}	-2.84×10^{6}	2.72×10	2.01×10^{3}	-8.77×10^{-4}	-1.37×10^{2}
1.2	7.3×10	-2.84×10^{6}	2.24×10	2.01×10^{3}	-5.81×10^{-4}	-7.3×10

The mean and maximum values of the DP total uncertainty are 1.19 and 1.94 kPa, and the mean estimation error of t_{max} is 7% at a POP of 5000 kPa.

Table 6

t_{max} at a POP of 5000 kPa.

ROD	0.2	0.4	0.6	1	1.2
Estimated value	119	134	133	126	139
Estimation error	15%	4.29%	5%	10%	0.71%

The $\dot{m}_{PL}$ is always equal to or greater than the discharged mass flow rate of the reference tank ($\dot{m}_{REF}$). The value of $\dot{m}_{PL}$ rises by an increase in the ROD; in fact, the difference between $\dot{m}_{PL}$ and $\dot{m}_{REF}$ grows which consequently raises the DP. The DP rises to a maximum value (DPS) and then drops due to the mass reduction of compressed gas inside the reference tank. The mean and maximum values of the standard deviation are 1.84 and 3.95 kPa respectively. The mean and maximum values of the DP estimation error are 0.8% and 6.1% respectively, and the mean and maximum values of the DP total uncertainty are 1.1 and 2.3 kPa respectively.

Table 7

Coefficients of Equation 1 at a POP of 7500 kPa.

ROD	*a*	*b*	*c*	*d*	*e*	*f*
0.2	-9.25×10	-3.57×10^{-2}	2.8	1.37×10^{9}	-2.3×10^{-4}	9.25×10
0.4	-9.45×10	-3.11×10^{-2}	3.11	1.37×10^{9}	-4.65×10^{-4}	9.45×10
0.6	-9.44×10	-3.35×10^{-2}	3.29	1.37×10^{9}	-3.32×10^{-4}	9.44×10
1	-9.49×10	-3.84×10^{-2}	3.45	1.37×10^{9}	-1.96×10^{-4}	9.49×10
1.4	-1.1×10^{2}	-3.55×10^{-2}	3.58	1.37×10^{9}	-3.76×10^{-4}	1.1×10^{2}

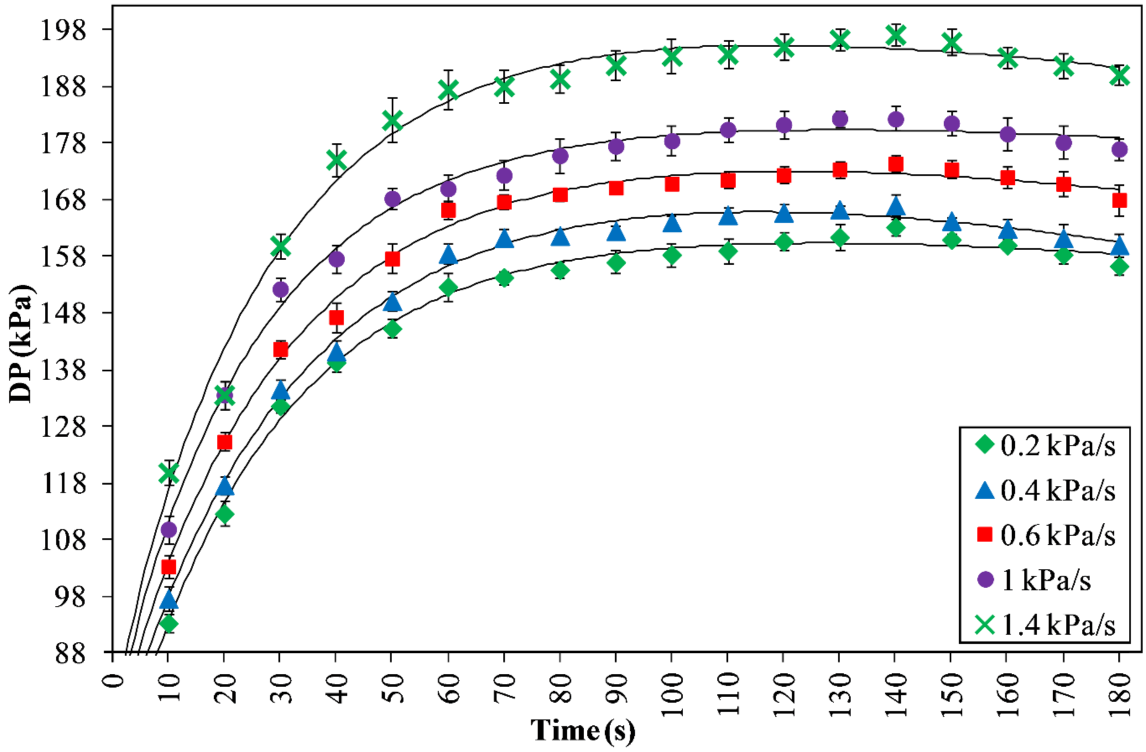

Figure 5

The DP versus time at a POP of 7500 kPa.

Table 8

t_{max} at a POP of 7500 kPa.

ROD	0.2	0.4	0.6	1	1.4
Estimated value	122	123	126	120	120
Estimation error	12.86%	12.14%	10%	14.29%	14.29%

The mean estimation error of t_{max} is 12.7% at a POP of 7500 kPa.

Table 9

Coefficients of Equation 1 at a POP of 9000 kPa.

ROD	*a*	*b*	*c*	*d*	*e*	*f*
0.2	-9.74×10	-3.97×10^{-2}	2.44	1.35×10^{9}	-2.74×10^{-4}	9.74×10
0.6	-9.78×10	-3.87×10^{-2}	2.69	1.3×10^{9}	-2×10^{-4}	9.78×10
0.8	-1.04×10^{2}	-4.02×10^{-2}	2.72	1.39×10^{9}	-1.97×10^{-4}	1.04×10^{2}
1.2	-1.15×10^{2}	-3.68×10^{-2}	1.41	1.36×10^{21}	-2.29×10^{-4}	1.15×10^{2}
1.6	-1.18×10^{2}	-3.86×10^{-2}	1.6	9.58×10^{19}	-2.45×10^{-4}	1.18×10^{2}

The mean and maximum values of the standard deviation are 2 and 3.5 kPa respectively. The mean and maximum values of the DP estimation error are also 0.62% and 1.92% respectively. Moreover, the mean and maximum values of the DP total uncertainty are 1.16 and 1.73 kPa, and the mean estimation error of t_{max} is 5.14% at a POP of 9000 kPa.

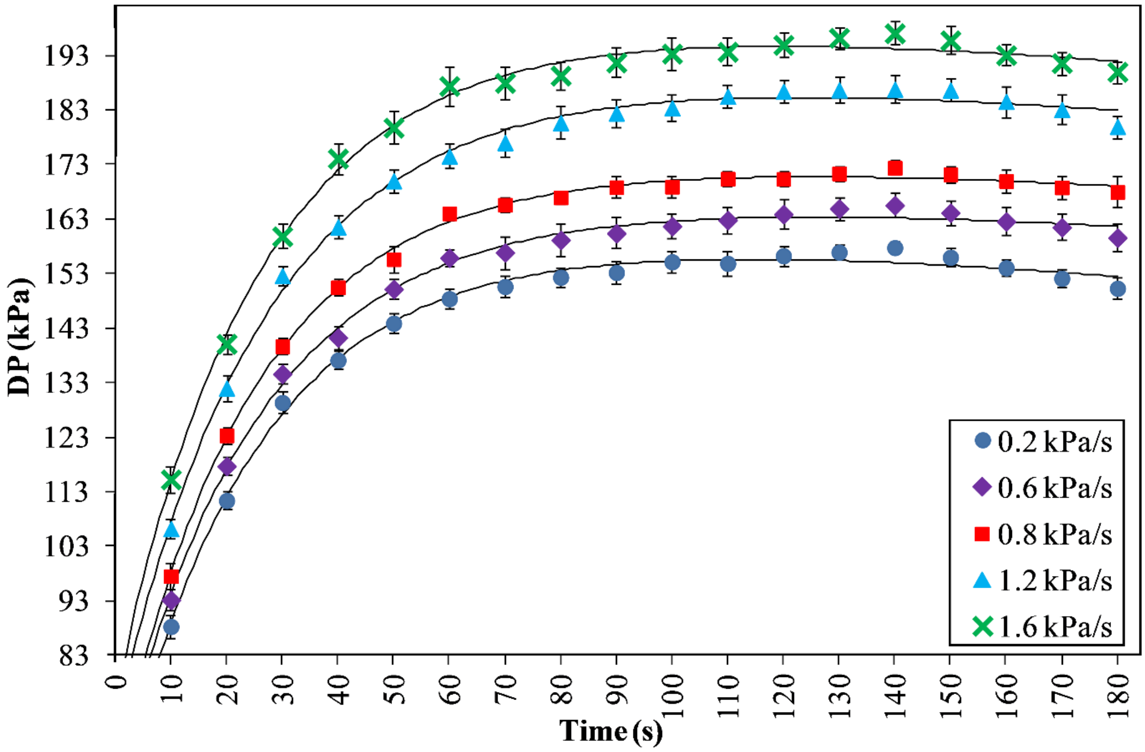

Figure 6

The DP versus time at a POP of 9000 kPa.

Table 10

t_{max} at a POP of 9000 kPa.

ROD	0.2	0.6	0.8	1.2	1.6
Estimated value	129	134	135	127	139
Estimation error	7.8%	4.29%	3.6%	9.3%	0.71%

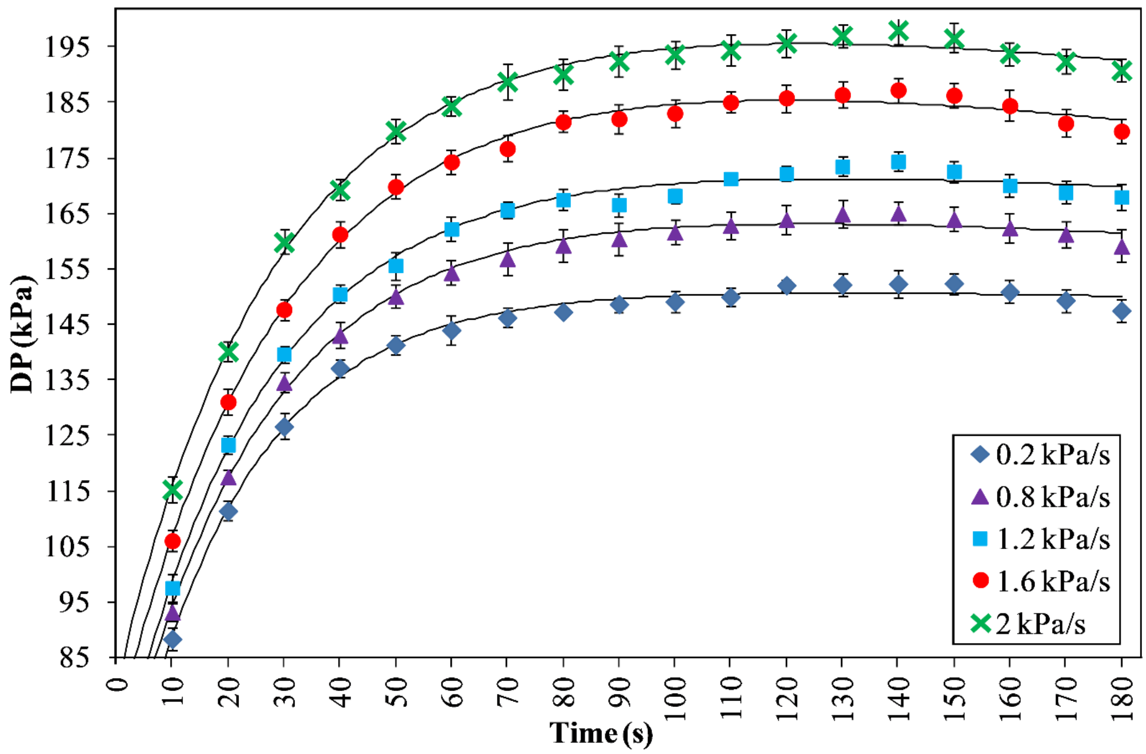

Figure 7

The DP versus time at a POP of 10500 kPa.

Table 11

Coefficients of Equation 1 at a POP of 10500 kPa.

ROD	*a*	*b*	*c*	*d*	*e*	*f*
0.2	-9.75×10	-4.6×10^{-2}	7.36×10^{-1}	1×10^{30}	-6.48×10^{-5}	9.75×10
0.8	-1.03×10^{2}	-3.89×10^{-2}	1.08	3.7×10^{23}	-1.62×10^{-4}	1.03×10^{2}
1.2	-1.07×10^{2}	-3.82×10^{-2}	1.19	3.89×10^{22}	-1.53×10^{-3}	1.07×10^{2}
1.6	-1.16×10^{2}	-3.34×10^{-2}	1.03	1×10^{30}	-3.24×10^{-4}	1.16×10^{2}
2	-1.17×10^{2}	-3.43×10^{-2}	1.15	1×10^{30}	-2.84×10^{-4}	1.17×10^{2}

The mean and maximum values of the standard deviation are 1.9 and 3.16kPa respectively. The mean and maximum values of the DP estimation error are also 0.7% and 2.5% respectively. Moreover, the mean and maximum values of the DP total uncertainty are 1.15 and 1.82 kPa respectively, and the mean estimation error of t_{max} is 9.71% at a POP of 10500 kPa.

Table 12

t_{max} at a POP of 10500 kPa.

ROD	0.2	0.8	1.2	1.6	2
Estimated Value	130	122	127	132	121
Estimation Error	7.14%	12.86%	9.29%	5.71%	13.57%

When the ROD parameter is constant, the only variable parameter is the POP. An increase in the POP intensifies collision between fluid molecules, which results in a rise in $\dot{m}_{REF}$; in fact, the velocity of the discharged compressed nitrogen gas through orifice grows when the POP rises. Therefore, the local pressure drops in orifice and the rate of the pressure drop in Route 3 approaches the rate of pressure drop in Route 2 (ROD). Thus, the difference between $\dot{m}_{PL}$ and $\dot{m}_{REF}$ decreases, and consequently the DP falls.

Figure 8 depicts the variation of the DPS versus ROD at different POP's. The rate of pressure drop in normal operating conditions is lower than the ROD at the same POP. Therefore, it is necessary to select an ROD higher than the rate of the pipeline pressure drop during a normal operation and lower than all the possible ROD's to regulate the ACV. The DPS results can be practically employed by applying a safety factor of 15% since nitrogen gas is used instead of natural gas and we have some uncertainties. In the case of a real gas pipeline rupture in which the ROD and the pipeline operating pressure (POP) are different from the experimental values obtained herein, new values can be found by applying interpolation to Figure 8.

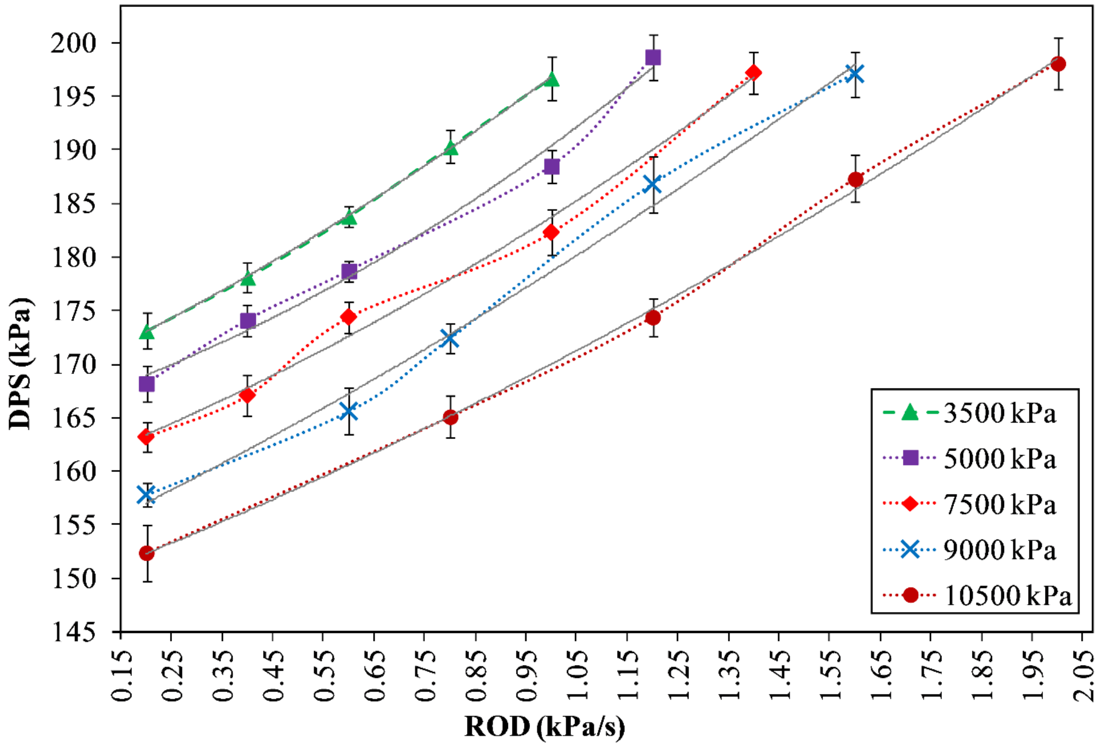

Figure 8

The DPS versus ROD at different POP's; gray continuous curves are estimations.

The maximum and the average percent of error of the DP estimation are 6.1% and 0.86% respectively in all the conditions. Furthermore, the maximum and average percent of error of the DPS estimation are 1.89% and 1.15% respectively in all the conditions. Equation 7 was developed for the DPS value estimation based on the ROD and POP. The constant parameters of *a*, *b*, and *c* of Equation 7 are presented in Table 13.

$$DPS = a(ROD)^2 + b(ROD) + \frac{(POP)}{c} \tag{7}$$

For example, the DPS and ROD can be determined at a specified POP. Each curve is denoted for a specified POP. A value can be selected for ROD bigger than the designed rate of the normal pipeline pressure drop. Finally, the DPS is determined by the indicated values of the POP and the ROD. For example, at a designed rate of the normal pipeline pressure drop equal to 0.65 kPa/s, the ROD can be selected as 0.85 kPa/s. At a POP of 5000 kPa and an ROD of 0.85 kPa/s, the DPS is determined to be 177 kPa. Accordingly, the spring of NC valve can be loaded for 150.45 kPa by adding a safety factor of 15%. The mentioned safety factor is based on the limited available data related to the practical conditions of ACV installation in gas transportation pipelines of Iran. The data confirm that a safety factor of 15% is sufficient and reliable for applying the findings of this paper to practical applications. The comparison between natural gas and nitrogen is presented in Table 15.

Table 13

Data analysis of the DPS estimation.

POP	*a*	*b*	*c*	R^2
3500	6.43	21.99	20.8	1
5000	9.71	15.11	30.2	0.989
7500	6.04	18.14	47	0.992
9000	3.76	22.47	59	0.992
10500	3.58	17.81	70.7	0.999

This safety factor is mainly related to the mass density; the mass density of natural gas and nitrogen in standard conditions (0 °C and 101.325 kPa) are 0.9 kg/m^3 and 1.2 kg/m^3 respectively.

Table 14

Data analysis of the DPS estimation.

POP	ROD	DPS	Estimated	Error	POP	ROD	DPS	Estimated	Error
3500	0.2	173.1	172.02	0.63%	5000	0.2	168.2	167.37	0.5%
	0.4	178.1	177.59	0.29%		0.4	174.1	172.84	0.79%
	0.6	183.8	182.1	0.93%		0.6	178.7	177.11	0.89%
	0.8	190.3	188.43	0.99%		1	188.5	186.7	0.95%
	1	196.7	194.4	1.17%		1.2	198.7	196.48	1.11%
7500	0.2	163.2	160.15	1.87%	9000	0.2	157.8	155	1.77%
	0.4	167.1	164.89	1.32%		0.6	165.6	163.17	1.46%
	0.6	174.4	172.56	1.05%		0.8	172.4	170.54	1.08%
	1	182.3	180.21	1.15%		1.2	186.8	184.97	0.98%
	1.4	197.2	194.65	1.29%		1.6	197.1	194.23	1.45%
10500	0.2	152.4	150.56	1.2%	10500	1.6	187.3	184.89	1.28%
	0.8	165.1	162.9	1.33%		2	198.1	199.1	1.46%
	1.2	174.4	171.1	1.89%					

Table 15

Comparison of the DPS of natural gas with that of nitrogen.

POP	ROD	DPS (Nitrogen)	DPS (Natural gas)	Safety factor
5000	1	188.5	166.7	11.6%
7500	1.4	197.2	170	13.8%

The DOP and RTP parameters are calculated by Equations 8 and 9 respectively using the experimental results in Table 14. The variation of the DOP versus the RTP at different POP's is delineated in Figure 9. The DOP can be defined by a linear equation (Equation 10) as a function of RTP at each POP. The constant parameters of *a* and *b* of Equation 10 are presented in Table 16.

$$DOP = {DPS}/{POP} \tag{8}$$

$$RTP = ROD \times {t_{\max}}/{POP} \tag{9}$$

$$DOP = a\left(RTP\right) + b \tag{10}$$

Table 16

Data analysis of the DOP estimation.

POP	Mean DOP	Error		*a*	*b*	R^2
		Average	Maximum			
3500	0.053	0.33%	1.07%	0.215	0.048	0.987
5000	0.04	0.62%	2.53%	0.179	0.033	0.954
7500	0.024	0.6%	1.92%	0.205	0.021	0.981
9000	0.019	0.73%	2.4%	0.223	0.016	0.984
10500	0.017	0.69%	1.63%	0.181	0.14	0.991

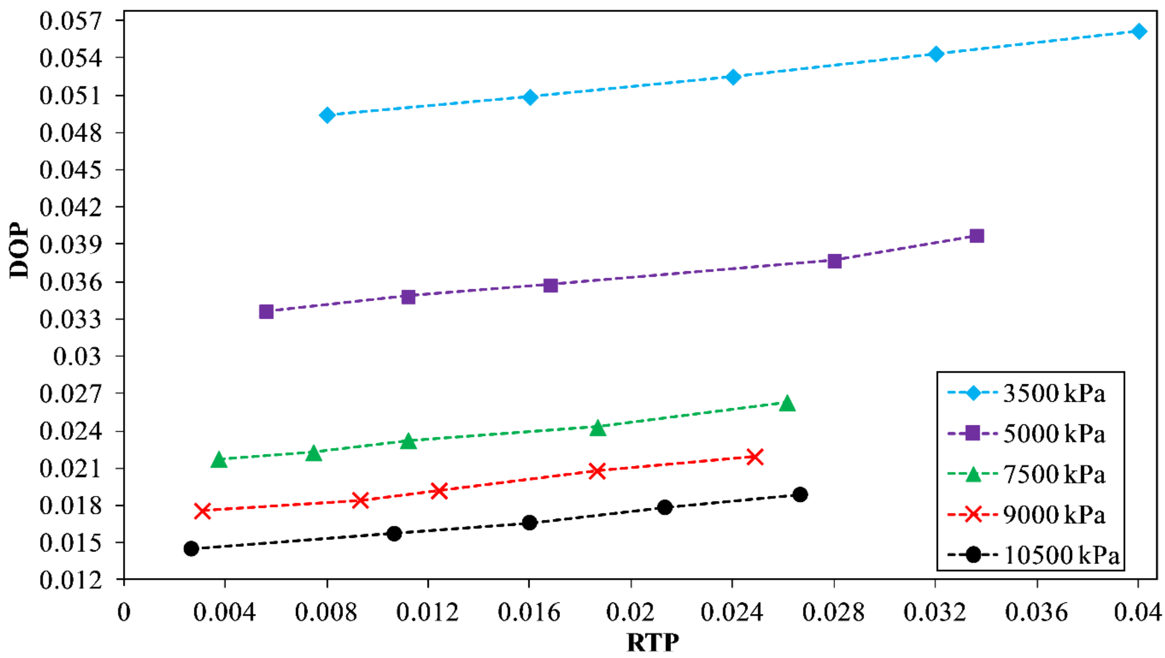

Figure 9

The DOP versus RTP at different POP's.

4. Conclusions

In the current work, the effect of parameters such as POP and ROD on the DPS of an automatic control valve was studied by performing 75 experimental tests, and statistical and uncertainty analyses were conducted. The compressed nitrogen gas was used instead of natural gas to avoid the hazardous conditions in presence of pressurized natural gas. The following conclusions are drawn based on our findings:

- The DP over a duration of 180 s is affected by the POP and the ROD. The DPS was increased by raising the ROD or decreasing the POP.
- The variation of DP with respect to time can be calculated using proposed Equation 1. The coefficients of this equation are presented in Tables 3, 5, 7, 9, and 11 in any conditions. In all the conditions, the mean of the maximum and average percent error of the DP estimation are 6.1% and 0.86% respectively.
- Equation 6 is proposed to estimate t_{max}. The mean percent error of this estimation is 7.35% in all the 25 conditions.
- The mean error of the DPS estimation using Equation 5 is 1.15%, and the maximum error is 1.89% at a POP of 10500 kPa and an ROD of 1.2 kPa/s.
- The DPS recommended herein can be practically employed by applying a safety factor of 15% to the experimental values in Figure 8.

The results in Figure 8 can be used for the value setting of automatic control valves installed on gas pipelines by applying a safety factor. Finally, the value setting (DPS) is determined by knowing the POP and the possible ROD in any specific condition in pipelines.

Acknowledgements

The authors acknowledge the financial support of the Research and Technology Center of the National Iranian Gas Company [Grant No. 950436 (2015)], Kiasa Company, and Ghaed Bassir Petrochemical Product Company.

Nomenclature

ACV	Automatic control valve
DOP	Non-dimensional DPS
DP	Differential pressure
DPS	Maximum DP value
NC Valve	Normally closed valve
POP	Pipeline operating pressure
ROD	Pipeline pressure drop rate
RTP	Non-dimensional
SD	Standard deviation
U	Uncertainty

References

Billmann, L. and Isermann, R., Leak Detection Methods for Pipelines, International Federation of Automatic Control Journal, Vol. 17, No. 2, p. 1813-1818, 1984.

Brunone, B. and Ferrante, M., Detecting Leaks in Pressurized Pipes by Means of Transients, Journal of Hydraulic Research, Vol. 39, p.1–9, 2002.

Chen, Y., Kuo, T., Kao, W., Tsai, J., Chen, W., and Fan, K., An Improved Method of Soil-gas Sampling for Pipeline Leak Detection: Flow Model Analysis and Laboratory Test, Journal of Natural Gas Science and Engineering, Vol. 42, p. 226-231, 2017.

Doostaregan, A., Automatic Line-break Control Valves and their Performances in Pipelines of Transmission, National Iranian Gas Company, Vol. 1, p.1-211, 2013 (In Persian).

Ebrahimi-Moghadam, A., Farzaneh-Gord, M., and Deymi-Dashtebayaz, M., Correlations for Estimating Natural Gas Leakage from Above-ground and Buried Urban Distribution Pipelines, Journal of Natural Gas Science and Engineering, Vol. 34, p.185-196, 2016.

Geiger, G., Werner, T., and Matko, D., Leak Detection and Locating: A Survey, Pipeline Simulation Interest Group, In proceedings of 35th Annual Meeting of PSIG, Bern, Switzerland, Paper No. 301, October 15–17, 2003.

Harriott, G.M., Gas Pipeline Simulation: Leak Detection, In Proceedings of 42nd Annual Meeting of the Pipeline Simulation Interest Group (PSIG), Houston, TX, 2011.

Lorusso, C., Line Break Detection System Analysis is Critical to Safer, More Economic Gas Pipeline Operations, 7th Pipeline Technology Conference, 2012.

Mahmoodi, M. and Gorji-Bandpy M., The Non-dimensional Diagram of Automatic Line-break Control Valve Performance Domain in Gas Transportation Pipeline, Iranian Society of Mechanical Engineering Journal, Vol. 19, No. 2, p. 41-59, 2017 (In Persian).

Mahmoodi, M. and Gorji-Bandpy, M., The Effective Parameters on Automatic Line-break Control Valve in Gas Transportation Pipelines, Vol. 34.3, No.2, p. 115-123, 2018 (In Persian).

Mahmoodi, M. and Gorji-Bandpy, M., An Experimental Study of the Effective Parameters on Automatic Line-break Control Valves Action in Natural Gas Pipelines, Journal of Natural Gas Science and Engineering, Vol. 52, p. 59-81, 2018.

Mahmoodi, M. and Gorji-Bandpy, M., Experimental Values for Adjusting an Automatic Control Valve in Gas Pipeline Transportation, Journal of Energy Equipment and Systems, Vol. 6, No. 2, p. 221-233, 2018.

Noguerol, R., Pipeline Control Modes and their Effect on Model-based Leak Detection, in proceedings of 42nd Annual Meeting of the Pipeline Simulation Interest Group (PSIG), Houston, TX, 2011.

Peekema, R.M., Causes of Natural Gas Pipeline Explosive Ruptures, Journal of Pipeline Systems Engineering and Practice, Vol. 4, No. 1, p.74-80, 2013.

Reddy, H.P., Narasimhan, S., Bhallamudi, S.M., and Bairagi, S., Leak Detection in Gas Pipeline Networks Using an Efficient State Estimator- Part II: Experimental and Field Evaluation, Computers and Chemical Engineering, Vol. 35, No. 4, p. 662-670, 2011.

Richards, F., Failure Analysis of a Natural Gas Pipeline Rupture, Journal of Failure Analysis and Prevention, Vol. 13, No. 6, p. 653-657, 2013.

Souza, A.L., Cruz, S.L., and Pereira, J.F.R., Leak Detection in Pipelines through Spectral Analysis of Pressure Signals, Brazilian Journal of Chemical Engineering, Vol. 17, p. 557–563, 2000.

Wang, W.L., Gao, Y.H., Lai, J.B., and Zhang, J.B., Setting of Pressure Drop Rate in Pipe Burst Detection System on Natural Gas Pipeline Block Valve, Gas Heat, Vol. 33, No. 7, p. 19-23, 2013.

Watanabe, K., and Himmelblau, D.M., Detection and Location of a Leak in a Gas-transport Pipeline by a New Acoustic Method, American Institute of Chemical Engineers Journal, Vol. 32, p. 1690-1701, 1980.

Yan, Y.T., Dong, X.Q., and Li, J.M., Experimental Study of Methane Diffusion in Soil for an Underground Gas Pipe Leak, Journal of Natural Gas Science and Engineering, Vol. 27, p. 82-89, 2015.

Zuo, L., Jiang, F., Jin, B., Zhang, L., and Xue, T., Value Setting for the Rate of Pressure Drop of Automatic Line-break Control Valves in Natural Gas Pipelines, Journal of Natural Gas Sciences and Engineering, Vol. 26, p. 803-809, 2015.

Zuo, L., Jiang, F., Jin, B., Zhang, L., and Xue, T., Influences on the Rate of Pressure Drop in Automatic Line Break Control Valves on a Natural Gas Pipeline, Journal of Natural Gas Sciences and Engineering, Vol. 26, p. 1489-1499, 2015.